

Neutral Four-Coordinate (Thiolato)- and (Selenolato)iron(II) Complexes: Synthesis and Characterization of $\text{Fe}(\text{E}-2,6\text{-}i\text{-Pr}_2\text{C}_6\text{H}_3)_2(1\text{-MeIm})_2$ ($\text{E} = \text{S}, \text{Se}$; $1\text{-MeIm} = 1\text{-Methylimidazole}$). Potential Models for a Biological, Mononuclear N_2S_2 Binding Site for Iron?

Cameron E. Forde, Alan J. Lough, Robert H. Morris,* and Ravindranath Ramachandran

Department of Chemistry, University of Toronto, 80 St. George Street, Toronto, Ontario, Canada M5S 1A1

Received September 22, 1995[⊗]

The complexes $\text{Fe}(\text{E}-2,6\text{-}i\text{-Pr}_2\text{C}_6\text{H}_3)_2(1\text{-MeIm})_2$ (**1**, $\text{E} = \text{S}$; **2**, $\text{E} = \text{Se}$; $1\text{-MeIm} = 1\text{-methylimidazole}$) are prepared by metathesis of chloride for 2,6-diisopropylbenzenethiolate or -selenolate from iron(II) chloride in the presence of 2 equiv of 1-methylimidazole. The complexes are very pale yellow (**1**) or pale orange (**2**), are oxygen sensitive, and have magnetic moments determined in solution at room temperature to be $4.6 \mu_{\text{B}}$ for both. The proton NMR spectra were completely assigned using line width and integration information and a deuterium labeling study using 1-methylimidazole-2,4,5- d_3 and 1-methylimidazole-2- d prepared by hydrothermal deuterium exchange reactions. Cyclic voltammetry studies of these compounds reveal complex irreversible oxidation behavior. Single-crystal X-ray diffraction studies for **1** at 296 K and for **2** at 173 K revealed distorted tetrahedral coordination geometries for both complexes. Complex **1** crystallizes in the monoclinic space group $P2_1/c$ with $a = 12.772(3) \text{ \AA}$, $b = 15.450(3) \text{ \AA}$, $c = 18.303(4) \text{ \AA}$, $\beta = 108.66(3)^\circ$, $Z = 4$, $V = 3421.8(13) \text{ \AA}^3$, $d_{\text{calc}} = 1.178 \text{ g cm}^{-3}$, $R = 0.0499$, and $R_w = 0.0523$. Complex **2** crystallizes in the monoclinic space group $P2_1/n$ with $a = 9.267(2) \text{ \AA}$, $b = 23.372(5) \text{ \AA}$, $c = 15.838(2) \text{ \AA}$, $\beta = 99.70(1)^\circ$, $Z = 4$, $V = 3381.3(11) \text{ \AA}^3$, $d_{\text{calc}} = 1.376 \text{ g cm}^{-3}$, $R = 0.0429$, and $R_w = 0.0739$.

Introduction

Histidine and cysteine are common ligands in bioinorganic systems. Two-cysteine, two-histidine coordination environments are known for zinc ions in zinc finger proteins¹ and the $[2\text{Fe}-2\text{S}]$ site of the Rieske center.^{2,3} This particular coordination environment has not been observed for a biological, mononuclear iron site. We are interested in determining the properties of four-coordinate iron complexes with a two-nitrogen, two-sulfur coordination sphere to explore the possibility that such a site might play a role in biological chemistry. We report the preparations and X-ray structure determinations of two such iron(II) complexes with 1-methylimidazole (to model histidine coordination) and 2,6-diisopropylbenzeneselenolate and -thiolate (to model cysteine coordination).

Structurally characterized neutral four-coordinate iron(II) complexes include the phosphine complexes with halide coligands $\text{FeBr}_2(\text{PET}_3)_2$ ⁴ and $\text{FeCl}_2(\text{dippe})_2$ ⁵ and complexes with a benzyl ligand, $\text{Fe}(\text{CH}_2\text{C}_6\text{H}_4\text{Me})_2(\text{dippe})_2$ ⁶ ($\text{dippe} = i\text{-Pr}_2\text{PCH}_2\text{CH}_2\text{-}i\text{-Pr}_2$), thiolate ligands, $\text{Fe}(\text{S}-2,4,6\text{-}i\text{-Pr}_3\text{C}_6\text{H}_2)_2(\text{SC}(\text{NMe}_2)_2)_2$,⁷ $\text{Fe}(\text{S}-2,4,6\text{-Me}_3\text{C}_6\text{H}_2)_2(\text{PMePh}_2)_2$,⁸ and $\text{Fe}(\text{S}-2,4\text{-}t\text{-Bu}_2\text{C}_6\text{H}_3)_2(\text{Ph}_2\text{PCH}_2\text{CH}_2\text{PPh}_2)_2$,⁸ and selenolate ligands, $\text{Fe}(\text{Se}-2,6\text{-}i\text{-Pr}_2\text{C}_6\text{H}_3)_2(\text{PMe}_2\text{Ph})_2$ and $\text{Fe}(\text{Se}-2,6\text{-}i\text{-Pr}_2\text{C}_6\text{H}_3)_2(\text{Et}_2\text{PCH}_2\text{CH}_2\text{PET}_2)_2$.⁹

A number of homoleptic four-coordinate iron(II) thiolate and selenolate ions have been prepared to model the iron site of the

reduced form of rubredoxins. For example, the structures of $(\text{PPh}_4)[\text{Fe}(\text{SPh})_4]^{10}$ and $(\text{NET}_4)_2[\text{Fe}(\text{SePh})_4]^{11}$ have been crystallographically characterized.

Experimental Section

General Information. Solvents for the preparation of **1** and **2** were dried and deoxygenated before use. Tetrahydrofuran, hexanes, and diethyl ether were dried over sodium and distilled from purple solutions of sodium-benzophenone ketyl under argon. The preparations of **1** and **2** were conducted in a Vacuum Atmospheres glovebox under a nitrogen atmosphere. Iron(II) chloride, 1-methylimidazole, chloroform- d , and benzene- d_6 were purchased from Aldrich. Deuterium oxide (99.92%) was a gift from Ontario Hydro. 2,6-Diisopropylphenyl bromide¹² and bis(2,6-diisopropylphenyl) diselenide⁹ were prepared by the published methods. Microanalysis of bis(2,6-diisopropylphenyl) disulfide was performed by Guelph Chemical Laboratories (Guelph, Ontario), and the analyses of **1** and **2** were performed by Canadian Microanalytical (Delta, BC) under inert-atmosphere conditions. ¹H and ¹³C NMR spectra were recorded on a Varian Gemini-200 spectrophotometer (at 200 MHz for ¹H and 50.3 MHz for ¹³C) and referenced internally to the residual solvent peak. The ²H NMR spectrum was recorded on a Varian 400 spectrometer at 61.4 MHz and referenced to the internal solvent peak. Electronic spectra were recorded on a Hewlett Packard 8452A diode array spectrophotometer in tetrahydrofuran in an anaerobic cell under nitrogen. Magnetic moments were determined in solution by Evans' method.¹³ A Bioanalytical Systems CV-1B electrochemical controller was used for cyclic voltammetric measurements in the inert-atmosphere glovebox. Solutions were 0.2 M for $n\text{-Bu}_4\text{NPF}_6$ in tetrahydrofuran. The electrode consisted of platinum working and counter electrodes and a silver reference electrode. Potentials are reported relative to the ferrocenium/ferrocene couple.

[⊗] Abstract published in *Advance ACS Abstracts*, April 1, 1996.

- Hanas, J. S.; Hazuda, D. J.; Bogenhagen, D. F.; Wu, F. H.; Wu, C. J. *Biol. Chem.* **1983**, *258*, 14120–14125.
- Kuila, D.; Schoonover, J. R.; Dyer, R. B.; Batie, C. J.; Ballou, D. P.; Fee, J. A.; Woodruff, W. H. *Biochim. Biophys. Acta* **1992**, *1140*, 175–183.
- Davidson, E.; Ohnishi, T.; Atta-Asafo-Adjei, E.; Daldal, F. *Biochemistry* **1992**, *31*, 3342–3351.
- Snyder, B. S.; Holm, R. H. *Inorg. Chem.* **1988**, *27*, 2339–2347.
- Hermes, A. R.; Girolami, G. S. *Inorg. Chem.* **1988**, *27*, 1775–1781.
- Hermes, A. R.; Girolami, G. S. *Organometallics* **1987**, *6*, 763–768.
- Bierbach, U.; Saak, W.; Haase, D.; Pohl, S. *Z. Naturforsch., B* **1991**, *46*, 1629–1634.
- Pohl, S.; Opitz, U.; Haase, D.; Saak, W. *Z. Anorg. Allg. Chem.* **1995**, *621*, 1140–1146.

- Forde, C. E.; Morris, R. H.; Ramachandran, R. *Inorg. Chem.* **1994**, *33*, 5647–5653.
- Coucovanis, D.; Swenson, D.; Baenziger, N. C.; Murphy, C.; Holah, D. G.; Sfarnas, N.; Simopoulos, A.; Kostikas, A. *J. Am. Chem. Soc.* **1981**, *103*, 3350–3362.
- McConnachie, J. M.; Ibers, J. A. *Inorg. Chem.* **1991**, *30*, 1770–1773.
- Schrock, R. R.; Wesoler, M.; Liu, A. H.; Wallace, K. C.; Dewan, J. C. *Inorg. Chem.* **1988**, *27*, 2050–2054.
- Evans, D. F. *J. Chem. Soc.* **1959**, 2003–2005.

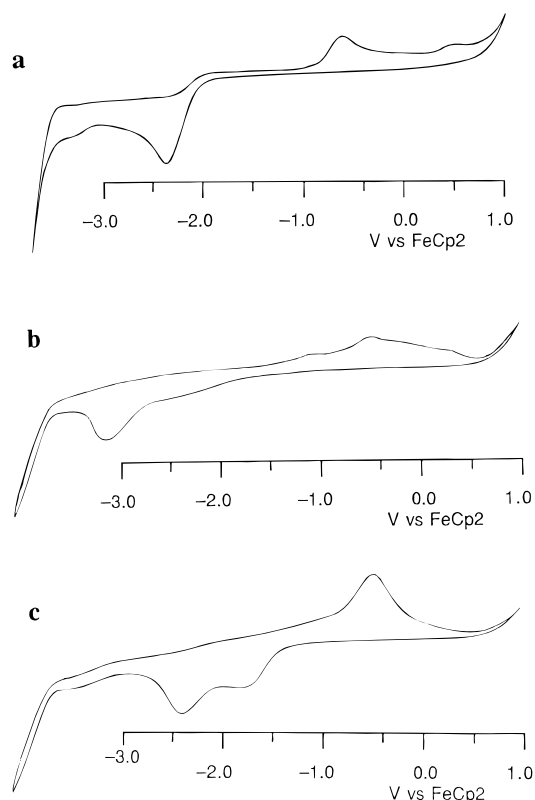


Figure 1. Cyclic voltammograms of (a) $S_2(2,6\text{-}i\text{-Pr}_2C_6H_3)_2$, (b) $Fe(S\text{-}2,6\text{-}i\text{-Pr}_2C_6H_3)_2(1\text{-MeIm})_2$, **1**, and (c) $Fe(Se\text{-}2,6\text{-}i\text{-Pr}_2C_6H_3)_2(1\text{-MeIm})_2$, **2**, 0.2 M $n\text{-Bu}_4NPF_6$ in THF under N_2 . Scan rate: 50 mV s^{-1} .

Bis(2,6-diisopropylphenyl) Disulfide. This compound was prepared in a manner similar to that reported for bis(2,6-diisopropylphenyl) diselenide.⁹ 2,6-Diisopropylphenyl bromide (10 g, 41.5 mmol) and magnesium metal (1.11 g, 45.7 mmol) in diethyl ether are heated to reflux (500 mL) under nitrogen overnight. The solution is cooled to room temperature, and elemental sulfur (1.5 g, 46.8 mmol) is added past a flow of nitrogen. This mixture is stirred overnight, after which an equal volume of ethanol with four pellets of KOH is added and dry air is bubbled through the solution for 1 day. This solution is reduced to dryness under vacuum, and the resulting oil is extracted with toluene (400 mL) and filtered through Celite. The filtrate is reduced to dryness under vacuum, and the resulting oil is dissolved in a minimum amount of diethyl ether. Crystals of $S_2(2,6\text{-}i\text{-Pr}_2C_6H_3)_2$ form on standing. Yield: 6.4 g (80%). Anal. Calcd for $C_{24}H_{34}S_2$: C, 74.55; H, 8.86. Found: C, 74.39; H, 8.96. 1H NMR (200 MHz, C_6D_6): δ 1.05 ppm (d, $CH(CH_3)_2$, $J = 6.8$ Hz), 3.85 (septet, $CHMe_2$, $J = 6.8$ Hz), 7.0–7.3 (m, m - and p - of $S\text{-}2,6\text{-}i\text{-Pr}_2C_6H_3$). ^{13}C NMR (50.3 MHz, C_6D_6): δ 24.06 ppm (s, $CH(CH_3)_2$), 31.76 (s, $CHMe_2$), 124.07 (s, m -), 130.59 (s, p -), 132.71 (s, o -), 153.90 (s, $ipso$). UV-vis (THF): λ 220 nm ($\epsilon = 18\,000\text{ M}^{-1}\text{ cm}^{-1}$), 261 (11 000), 322 (1900). EI-MS (m/e): calcd for $C_{24}H_{34}S_2$ 386.65; found 386 $[M]^+$, 193 $[ArS]^+$, 162 $[Ar]^+$. The pattern of the parent ion mass peaks was successfully modeled with the natural-abundance isotope ratios. Cyclic voltammetry (vs Fc^+/Fc , THF): irreversible oxidation at -0.64 V, irreversible reduction at -2.31 V; see Figure 1.

1-Methylimidazole-2,4,5- d_3 . Deuteration of the ring protons of 1-methylimidazole is performed in a manner similar to the reported preparation of imidazole- d_3 .¹⁴ 1-Methylimidazole (1.030 g) is dissolved in D_2O (24 mL, 99.92%) and sealed in a Teflon-lined steel reaction chamber. This vessel is heated to $250\text{ }^\circ\text{C}$ for 4 h and then cooled to room temperature. Water is removed by simple distillation and the product isolated by vacuum distillation. Assignment of the signals was made in accord with signals reported for the protonated compound.¹⁵ 1H NMR (200 MHz, $CDCl_3$): δ 3.70 (s, NCH_3). ^{13}C NMR (50.3 MHz, $CDCl_3$): δ 137.6 ppm (1:1:1 t, 2-C, $^1J_{CD} = 32$ Hz), 129.2 (1:1:1 t, 4-C, $^1J_{CD} = 29$), 119.7 (1:1:1 t, 5-C, $^1J_{CD} = 29$), 33.2 (s, NCH_3).

(14) Gillespie, R. J.; Grimison, A.; Ridd, J. H.; White, R. F. M. *J. Chem. Soc.* **1958**, 3228–3229.

1-Methylimidazole-2- d . 1-Methylimidazole (1.20 g, 14.6 mmol) is dissolved in D_2O (24 mL, 99.92 atom %) and sealed in a Teflon-lined steel reaction chamber. This vessel is heated to $150\text{ }^\circ\text{C}$ for 1.5 h and then cooled to room temperature. The water is removed by simple distillation, and the residue is distilled under vacuum. Residual protonation of the 2-position (δ 7.3 ppm) was determined by 1H NMR to be 4%. 1H NMR (200 MHz, $CDCl_3$): δ 7.04 ppm (s, 5- H), 6.88 (s, 4- H), 3.68 (s, NCH_3). ^{13}C NMR (50.3 MHz, $CDCl_3$): δ 137.64 ppm (1:1:1 t, 2-C, $^1J_{CD} = 31$ Hz), 129.45 (s, 4-C), 120.12 (s, 5-C), 33.35 (s, NCH_3).

$Fe(S\text{-}2,6\text{-}i\text{-Pr}_2C_6H_3)_2(1\text{-MeIm})_2$, **1. Sodium borohydride is added in several small portions to a solution of $S_2(2,6\text{-}i\text{-Pr}_2C_6H_3)_2$ (198 mg; 0.512 mmol) in tetrahydrofuran–ethanol (1:1, 20 mL) until the solution is colorless. The resulting solution is filtered and added dropwise to a stirred solution of iron(II) chloride (65 mg, 0.513 mmol) and 1-methylimidazole (84 mg, 1.02 mmol) in tetrahydrofuran (100 mL). This solution is stirred for 1 h, and the volatile components are removed under vacuum. The resulting oil is extracted with toluene (100 mL) and filtered through Celite. The toluene is removed under vacuum, and the powder is dissolved in a minimum amount of diethyl ether (20 mL). This solution is cooled to $-30\text{ }^\circ\text{C}$ overnight, and pale yellow crystals are collected. Yield: 239 mg (77%). Anal. Calcd for $C_{32}H_{46}FeN_4S_2$: C, 63.35; H, 7.64; N, 9.23. Found: C, 63.87; H, 7.52; N, 9.26. 1H NMR (200 MHz, C_6D_6): δ 63.3 ppm (s, 2- H of methylimidazole), 44.6 (s, 4- H), 24.8 (s, m -), 20.0 (s, $CHMe_2$), 13.4 (s, NCH_3), 9.0 (s, $CH(CH_3)_2$), 1.7 (s, 5- H), -30.0 (s, p -). UV-vis (THF): λ 292 nm ($\epsilon = 11\,700\text{ M}^{-1}\text{ cm}^{-1}$), 268 (9600). Electrochemistry (vs Fc^+/Fc , THF, 50 mV s^{-1}): see Figure 1.**

$Fe(S\text{-}2,6\text{-}i\text{-Pr}_2C_6H_3)_2(1\text{-MeIm-}2,4,5\text{-}d_3)_2$, **1- d_6 . The preparation of this compound was performed as for the preparation of **1** except 1-methylimidazole-2,4,5- d_3 was used. 2H NMR (61 MHz, C_7H_8): δ 62.0 ppm (s, 2- D), 43.0 (s, 4- D), 0.7 (s, 5- D).**

$Fe(S\text{-}2,6\text{-}i\text{-Pr}_2C_6H_3)_2(1\text{-MeIm-}2\text{-}d)_2$, **1- d_2 . The preparation of this compound was performed as for the preparation of **1** except 1-methylimidazole-2- d was used. 1H NMR (200 MHz, C_6D_6): δ 38.2 ppm (s, 4- H of methylimidazole), 24.3 (s, m -), 19.3 (br s, $CHMe_2$), 13.2 (s, NCH_3), 8.4 (s, $CH(CH_3)_2$), 1.0 (s, 5- H), -30.5 (s, p -).**

$Fe(Se\text{-}2,6\text{-}i\text{-Pr}_2C_6H_3)_2(1\text{-MeIm})_2$, **2. The preparation of **2** was performed in the same manner as that for **1** with the substitution of $Se_2(2,6\text{-}i\text{-Pr}_2C_6H_3)_2$ for the disulfide. Yield: 80%. Anal. Calcd for $C_{32}H_{46}FeN_4Se_2$: C, 54.87; H, 6.62; N, 8.00. Found: C, 54.35; H, 6.27; N, 7.97. 1H NMR (200 MHz, C_6D_6): δ 66.2 ppm (s, 4- H of methylimidazole), 48.6 (s, 2- H), 18.1 (s, m -), 15.7 (s, $CHMe_2$), 12.0 (s, NCH_3), 7.8 (s, $CH(CH_3)_2$), 0.7 (s, 5- H), -18.9 (s, p -). UV-vis (THF): λ 220 nm ($\epsilon = 28\,000\text{ M}^{-1}\text{ cm}^{-1}$), 248 (14 000), 290 (9000), 364 (3000). Electrochemistry (vs Fc^+/Fc , THF, 50 mV s^{-1}): see Figure 1.**

X-ray Structural Characterization of **1 and **2**.** A summary of selected crystallographic data is given in Table 1. Data, for both compounds, were collected using Mo $K\alpha$ radiation ($\lambda = 0.710\,73\text{ \AA}$). For each compound, the intensities of three standard reflections measured periodically showed no decay. The data were corrected for Lorentz and polarization effects and for absorption¹⁶ (minimum and maximum transmission coefficients were 0.213 and 0.257 for **1** and 0.435 and 0.824 for **2**).

The structures were solved and refined using the SHELXTL/PC¹⁷ package. For both structures all non-hydrogen atoms were refined with anisotropic thermal parameters. The weighting schemes were $w^{-1} = [\sigma^2(F_o) + 0.0004F_o^2]$ for **1** and $w^{-1} = [\sigma^2(F_o) + (0.0261P)^2 + 1.26P]$ where $P = (F_o^2 + 2F_c^2)/3$ for **2**. Hydrogen atoms were included in calculated positions and treated as riding atoms. Selected bond lengths and angles for **1** and **2** are given in Table 2.

Results and Discussion

Preparation. Metathesis of chloride ions from iron(II) chloride with 2,6-diisopropylbenzenethiolate or -selenolate in

(15) Pugmire, R. J.; Grant, D. M.; Townsend, L. B.; Robins, R. K. *J. Am. Chem. Soc.* **1973**, *95*, 2791–2796.

(16) Sheldrick, G. M. SHELXA-90: Program for absorption correction. University of Göttingen, Germany.

(17) Sheldrick, G. M. SHELXTL/PC V5.0. Siemens Analytical X-ray Instruments Inc., Madison, WI.

Table 1. Summary of Crystallographic Parameters for Fe(S-2,6-*i*-Pr₂C₆H₃)₂(1-MeIm)₂, **1**, and Fe(Se-2,6-*i*-Pr₂C₆H₃)₂(1-MeIm)₂, **2**

	1	2
empirical formula	C ₃₂ H ₄₆ FeN ₄ S ₂	C ₃₂ H ₄₆ FeN ₄ Se ₂
fw	606.71	700.50
crystal size	0.42, 0.34, 0.39	0.42, 0.34, 0.54
crystal system	monoclinic	monoclinic
space group	<i>P</i> 2 ₁ / <i>c</i>	<i>P</i> 2 ₁ / <i>n</i>
<i>a</i> , Å	12.772(3)	9.267(2)
<i>b</i> , Å	15.450(3)	23.372(5)
<i>c</i> , Å	18.303(4)	15.838(2)
β, deg	108.66(3)	99.70(1)
<i>V</i> , Å ³	3421.8(13)	3381.3(11)
<i>Z</i>	4	4
<i>d</i> _{calc} , g cm ⁻³	1.178	1.376
abs coeff, mm ⁻¹	3.81	2.83
temp, K	294(2)	173(2)
diffractometer	Enraf-Nonius CAD-4	Siemens P4
min, max 2θ, deg	4.0, 54.0	5.0, 54.0
no. of refls colld	7978	7738
no. of indep refls	7450	7296
no. of obs refls [<i>F</i> > 4.0σ(<i>F</i>)]	3116	4752
<i>R</i> _{int}	0.020	0.035
no. of params	354	364
refinement on	<i>F</i>	<i>F</i> ²
<i>R</i> indices (obs data)	<i>R</i> = 0.0499, <i>R</i> _w = 0.0523 ^a	<i>R</i> ₁ = 0.0429, <i>R</i> _{2w} = 0.0739 ^b
<i>R</i> indices (all data)	<i>R</i> = 0.1457, <i>R</i> _w = 0.0640 ^a	<i>R</i> ₁ = 0.0922, <i>R</i> _{2w} = 0.0890 ^b
min, max peak in Δ <i>F</i> map, e Å ⁻³	-0.22, 0.50	-0.40, 0.41

^a *R* = Σ(*F*_o - *F*_c)/Σ(*F*_o), *R*_w = [Σw(*F*_o - *F*_c)²/Σw(*F*_o)²]^{1/2}. ^b *R*₁ = Σ(*F*_o - *F*_c)/Σ(*F*_o), *R*_{2w} = [Σ[w(*F*_o² - *F*_c²)]/Σ[w(*F*_o²)]^{1/2}.

Table 2. Selected Bond Lengths (Å) and Angles (deg) for Fe(S-2,6-*i*-Pr₂C₆H₃)₂(1-MeIm)₂, **1**, and Fe(Se-2,6-*i*-Pr₂C₆H₃)₂(1-MeIm)₂, **2**

	1	2	
Fe-S(1)	2.311(2)	Fe-Se(1)	2.4329(7)
Fe-S(2)	2.321(1)	Fe-Se(2)	2.4557(8)
Fe-N(1)	2.095(4)	Fe-N(1)	2.063(3)
Fe-N(3)	2.073(4)	Fe-N(3)	2.075(3)
S(1)-C(9)	1.778(4)	Se(1)-C(9)	1.942(4)
S(2)-C(21)	1.781(4)	Se(2)-C(21)	1.940(4)
N(1)-C(1)	1.317(7)	N(1)-C(1)	1.323(5)
N(1)-C(3)	1.356(7)	N(1)-C(3)	1.381(5)
N(2)-C(1)	1.322(7)	N(2)-C(1)	1.347(5)
N(2)-C(2)	1.332(9)	N(2)-C(2)	1.361(5)
N(2)-C(4)	1.461(8)	N(2)-C(4)	1.460(5)
C(2)-C(3)	1.323(11)	C(2)-C(3)	1.352(6)
N(3)-C(5)	1.304(6)	N(3)-C(5)	1.325(5)
N(3)-C(7)	1.350(8)	N(3)-C(7)	1.383(5)
N(4)-C(5)	1.324(8)	N(4)-C(5)	1.339(5)
N(4)-C(6)	1.346(9)	N(4)-C(6)	1.374(5)
N(4)-C(8)	1.455(7)	N(4)-C(8)	1.458(5)
C(6)-C(7)	1.341(7)	C(6)-C(7)	1.350(6)
S(1)-Fe-S(2)	116.4(1)	Se(1)-Fe-Se(2)	110.99(3)
N(1)-Fe-N(3)	97.2(2)	N(1)-Fe-N(3)	98.32(13)
N(1)-Fe-S(1)	106.0(1)	N(1)-Fe-Se(1)	105.09(9)
N(1)-Fe-S(2)	114.0(1)	N(1)-Fe-Se(2)	114.21(9)
N(3)-Fe-S(1)	108.8(1)	N(3)-Fe-Se(1)	112.23(9)
N(3)-Fe-S(2)	112.6(1)	N(3)-Fe-Se(2)	115.04(9)
Fe-S(1)-C(9)	103.1(2)	Fe-Se(1)-C(9)	98.46(11)
Fe-S(2)-C(21)	101.4(1)	Fe-Se(2)-C(21)	103.86(11)
Fe-N(1)-C(1)	130.0(3)	Fe-N(1)-C(1)	127.3(3)
Fe-N(1)-C(3)	125.9(4)	Fe-N(1)-C(3)	126.8(3)
Fe-N(3)-C(5)	130.4(4)	Fe-N(3)-C(5)	128.7(3)
Fe-N(3)-C(7)	126.3(3)	Fe-N(3)-C(7)	124.3(3)
C(1)-N(1)-C(3)	104.1(5)	C(1)-N(1)-C(3)	105.9(3)
C(5)-N(3)-C(7)	103.3(4)	C(5)-N(3)-C(7)	104.9(3)

the presence of 2 equiv of 1-methylimidazole produces Fe(E-2,6-*i*-Pr₂C₆H₃)₂(1-MeIm)₂ (E = S (**1**); Se (**2**)). The 2,6-diisopropylbenzenethiolato and -selenolato anions were generated by reduction of the corresponding disulfide or diselenide with sodium borohydride. We have previously reported the effectiveness of this method in the preparation of Fe(Se-2,6-*i*-Pr₂C₆H₃)₂(L)₂ [(L)₂ = (PMe₂Ph)₂, depe].⁹

Table 3. Atomic Coordinates (× 10⁴) and Equivalent Isotropic Displacement Coefficients (Å² × 10³) for Fe(S-2,6-*i*-Pr₂C₆H₃)₂(1-MeIm)₂, **1**

	<i>x</i>	<i>y</i>	<i>z</i>	<i>U</i> (eq) ^a
Fe	6546(1)	7900(1)	1544(1)	50(1)
S(1)	5351(1)	7269(1)	2105(1)	59(1)
S(2)	7353(1)	9198(1)	2077(1)	55(1)
N(1)	7685(3)	6937(3)	1512(2)	57(2)
N(2)	9190(4)	6234(3)	1556(3)	67(2)
N(3)	5761(3)	7987(3)	365(2)	64(2)
N(4)	4555(4)	8227(3)	-778(3)	69(2)
C(1)	8748(4)	6996(3)	1605(3)	60(2)
C(2)	8374(7)	5658(4)	1417(4)	98(4)
C(3)	7464(5)	6080(4)	1397(4)	89(3)
C(4)	10345(5)	6072(4)	1625(4)	102(3)
C(5)	4797(5)	8304(3)	-22(3)	67(3)
C(6)	5423(5)	7826(5)	-895(3)	99(3)
C(7)	6154(5)	7694(5)	-192(3)	99(3)
C(8)	3547(5)	8482(4)	-1380(3)	110(3)
C(9)	4028(3)	7585(3)	1483(3)	49(2)
C(10)	3620(4)	8419(3)	1516(3)	60(2)
C(11)	2570(5)	8619(4)	1026(4)	83(3)
C(12)	1940(5)	8028(5)	513(4)	95(3)
C(13)	2346(4)	7221(4)	481(3)	81(3)
C(14)	3394(4)	6980(3)	951(3)	55(2)
C(15)	4261(4)	9093(4)	2073(3)	76(3)
C(16)	4254(7)	9960(5)	1715(4)	165(5)
C(17)	3876(5)	9166(5)	2776(4)	118(4)
C(18)	3783(4)	6077(4)	866(4)	75(3)
C(19)	3102(6)	5386(4)	1055(5)	145(5)
C(20)	3870(6)	5922(4)	78(5)	142(5)
C(21)	8776(3)	8906(3)	2429(3)	43(2)
C(22)	9476(4)	9135(3)	2004(3)	52(2)
C(23)	10558(4)	8839(3)	2265(3)	67(3)
C(24)	10956(4)	8361(4)	2916(4)	77(3)
C(25)	10280(4)	8176(3)	3343(3)	67(2)
C(26)	9195(3)	8447(3)	3119(3)	51(2)
C(27)	9065(5)	9662(4)	1270(3)	76(3)
C(28)	9843(7)	10383(5)	1253(4)	168(5)
C(29)	8873(7)	9139(5)	573(4)	144(5)
C(30)	8506(4)	8227(3)	3629(3)	66(2)
C(31)	9025(5)	8570(4)	4448(3)	100(3)
C(32)	8284(5)	7259(4)	3639(3)	84(3)

^a Equivalent isotropic *U* defined as one-third of the trace of the orthogonalized *U*_{ij} tensor.

Characterization. These complexes are formally 14-electron, coordinatively unsaturated complexes and are oxygen sensitive both in solution and in the solid state. A variety of physical methods have been used to characterize these complexes, including elemental analysis, magnetic moment determinations, cyclic voltammetry, proton NMR, UV-vis spectroscopy, and single-crystal X-ray diffraction.

Ultraviolet-Visible Spectroscopy. Crystals of bis(2,6-diisopropylphenyl) disulfide have a pale yellow color due to an intense absorption in the ultraviolet region which tails off into the visible spectrum. Complexes **1** and **2** absorb weakly in the visible region, and the crystals have pale yellow and pale orange colorations, respectively. For compound **1**, absorptions are observed at 292 and 268 nm with molar absorptivities of 11 700 and 9600 M⁻¹ cm⁻¹, respectively. For compound **2**, absorptions are observed at the following wavelengths (molar absorptivities): 220 nm (28 000 M⁻¹ cm⁻¹), 248 (14 000), 290 (9000), 364 (3000).

Cyclic Voltammetry. The voltammograms, after several cycles (-0.6 to -4.0 to +1.0 to -0.6 V, at 50 mV/s), of the bis(2,6-diisopropylphenyl) disulfide and the metal complexes **1** and **2** in THF are shown in Figure 1. The free disulfide reduces irreversibly to the thiolate at -2.31 V vs Cp₂Fe⁺⁰ and then oxidizes back to the disulfide irreversibly at -0.64 V. Similar behavior has been reported for diphenyl diselenide and diphenyl disulfide¹⁸ as well as bis(2,6-diisopropylphenyl) diselenide.⁹ Compounds **1** and **2** exhibit complex electrochemical behavior.

Table 4. Atomic Coordinates ($\times 10^4$) and Equivalent Isotropic Displacement Coefficients ($\text{\AA}^2 \times 10^3$) for $\text{Fe}(\text{Se}-2,6\text{-}i\text{-Pr}_2\text{C}_6\text{H}_3)_2\text{-}(1\text{-MeIm})_2$, **2**

	x	y	z	$U(\text{eq})^a$
Fe	5072(1)	1511(1)	5973(1)	23(1)
Se(1)	5986(1)	531(1)	6252(1)	25(1)
Se(2)	6877(1)	2209(1)	6612(1)	25(1)
N(1)	4531(3)	1568(1)	4658(2)	26(1)
N(2)	3889(4)	1342(1)	3299(2)	30(1)
N(3)	2992(3)	1620(1)	6271(2)	28(1)
N(4)	961(3)	1439(2)	6772(2)	31(1)
C(1)	4083(4)	1150(2)	4113(3)	29(1)
C(2)	4235(5)	1908(2)	3327(3)	34(1)
C(3)	4626(4)	2049(2)	4162(3)	31(1)
C(4)	3408(6)	996(2)	2536(3)	49(1)
C(5)	2420(4)	1383(2)	6899(3)	28(1)
C(6)	555(5)	1722(2)	6009(3)	38(1)
C(7)	1806(5)	1829(2)	5707(3)	36(1)
C(8)	-22(5)	1206(2)	7314(3)	45(1)
C(9)	4791(4)	315(2)	7096(2)	26(1)
C(10)	5252(5)	472(2)	7963(3)	32(1)
C(11)	4358(5)	313(2)	8551(3)	42(1)
C(12)	3075(6)	27(2)	8307(3)	48(1)
C(13)	2640(5)	-127(2)	7459(3)	44(1)
C(14)	3490(4)	8(2)	6841(3)	30(1)
C(15)	6682(5)	782(2)	8281(3)	37(1)
C(16)	6554(6)	1276(2)	8878(4)	61(2)
C(17)	7864(6)	372(2)	8662(4)	70(2)
C(18)	2963(5)	-174(2)	5918(3)	34(1)
C(19)	2270(5)	-772(2)	5824(3)	45(1)
C(20)	1888(5)	270(2)	5452(3)	42(1)
C(21)	6016(4)	2939(2)	6222(2)	24(1)
C(22)	4912(4)	3181(2)	6634(2)	26(1)
C(23)	4400(5)	3724(2)	6386(3)	39(1)
C(24)	4930(5)	4026(2)	5756(3)	43(1)
C(25)	5980(5)	3786(2)	5349(3)	37(1)
C(26)	6539(4)	3243(2)	5568(2)	28(1)
C(27)	4329(4)	2889(2)	7361(3)	32(1)
C(28)	5192(5)	3078(2)	8226(3)	44(1)
C(29)	2691(5)	2981(2)	7331(3)	45(1)
C(30)	7734(4)	3005(2)	5120(2)	32(1)
C(31)	9240(5)	3184(2)	5598(3)	44(1)
C(32)	7601(5)	3186(2)	4177(3)	44(1)

^a Equivalent isotropic U defined as one-third of the trace of the orthogonalized U_{ij} tensor.

Magnetic Moments and NMR Spectroscopy. The magnetic moments of complexes **1** and **2** were determined in solution by Evans' Method¹³ to be $4.6 \mu_B$ (correction for ligand diamagnetism was made). This value is lower than the calculated spin-only value of $4.9 \mu_B$.

The ¹H NMR spectra of these complexes (Figure 2) exhibit broadening and shifting of the resonances due to the unpaired electron density at the iron centers. The resonances for complex **1** span a range of +63 to -30 ppm, while complex **2** gives rise to resonances that span a range from +66 to -20 ppm.

Complete unambiguous assignment of the spectra is possible using a combination of line width and integration analyses as well as a deuterium-labeling study (Figure 2). The ¹H NMR spectrum recorded of the complex prepared from 1-methylimidazole-2-*d*, **1-d**₂, has all the signals of **1** except for a signal around 65 ppm (not shown). This spectrum also exhibits isotopic shifts of the imidazole ring protons. The resonance for the proton in the 4-position of **1-d**₂ is shifted 6.4 ppm upfield relative to that of **1**, while the proton at the 5-position is shifted 0.7 ppm upfield. The ²H NMR spectrum of the complex prepared from 1-methylimidazole-2,4,5-*d*₃, **1-d**₆, exhibits resonances for the imidazole ring deuterons at 62.0, 43.0, and 0.7 ppm for the 2-, 4-, and 5-positions, respectively; these positions are consistent with the assignments given in Figure 2.

There are marked differences in the ¹H NMR spectra of **1** and **2**, despite the similarities of the two structures. The largest difference appears in the chemical shifts of the meta (24.8 vs 18.1 ppm) and the para (-30.0 vs -18.9 ppm) protons (for **1**

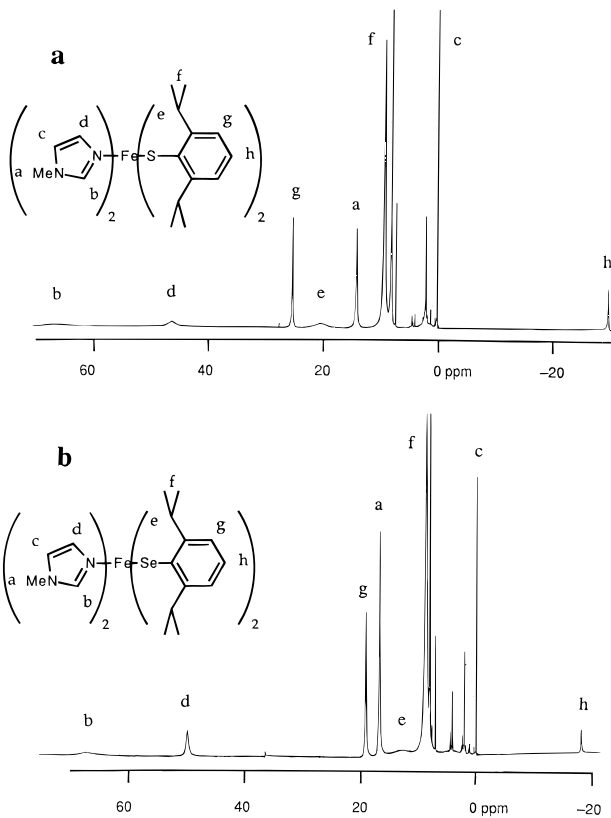


Figure 2. 300 MHz ¹H NMR spectra of (a) $\text{Fe}(\text{S}-2,6\text{-}i\text{-Pr}_2\text{C}_6\text{H}_3)_2(1\text{-MeIm})_2$, **1**, and (b) $\text{Fe}(\text{Se}-2,6\text{-}i\text{-Pr}_2\text{C}_6\text{H}_3)_2(1\text{-MeIm})_2$, **2**, in C_6D_6 at 295 K.

and **2**, respectively). The paramagnetic shift is composed of isotropic and contact terms. There is an alternation in the sign of the paramagnetic shift for the protons of the aromatic rings: upfield shifts are observed for ortho and para protons, while meta protons are shifted downfield. This is attributed to a through-bond, or contact, mechanism. The through-space interaction, or pseudocontact mechanism, is indiscriminate, and downfield shifts result. Comparing the magnitude of the paramagnetic shift for the aromatic ring protons in **1** and **2** reveals larger shifts for compound **1**. The increase in the upfield shift of the para proton of the thiolate ligand over the selenolate ligand reflects the nature of the bonding between the metal and these ligands since the upfield shifts are due to the contact mechanism. The larger contact shifts in **1** imply better orbital overlap in the Fe-S case.

The difference in the methine proton chemical shifts of compounds **1** and **2** is another interesting feature. The methine proton on the selenolate ligand in **2** resonates at 15.7 ppm, while that of the thiolate ligand in **1** resonates at 20.0 ppm. The methine protons of the closely related compounds $\text{Fe}(\text{Se}-2,6\text{-}i\text{-Pr}_2\text{C}_6\text{H}_3)_2(\text{L})_2$ [$(\text{L})_2 = (\text{PMe}_2\text{Ph})_2, \text{Et}_2\text{PCH}_2\text{CH}_2\text{PEt}_2$] are observed at 20.6 and 19.2 ppm, respectively. The structure of **2** may differ in solution from that of the other related complexes. This difference may be a greater separation between the methine protons and the iron atom as a greater separation between the iron and the methine protons is observed in the solid state structure determination.

Structural Studies. The coordination environment about the iron center in **1** is distorted tetrahedral (Figure 3). The largest angle, $\text{S}(1)\text{FeS}(2)$, is $116.5(1)^\circ$, while the narrowest angle, $\text{N}(1)\text{-FeN}(3)$, is $97.2(2)^\circ$. The Fe-S separations are 2.321(1) and 2.312(2) Å. The Fe-N separations are 2.095(4) and 2.070(4) Å. The structure of **2** is also distorted from tetrahedral (Figure 4). The $\text{Se}(1)\text{FeSe}(2)$ angle is $110.99(3)^\circ$, while the $\text{N}(1)\text{FeN}(3)$ angle is $98.32(13)^\circ$. The Fe-Se separations are 2.4329(7)

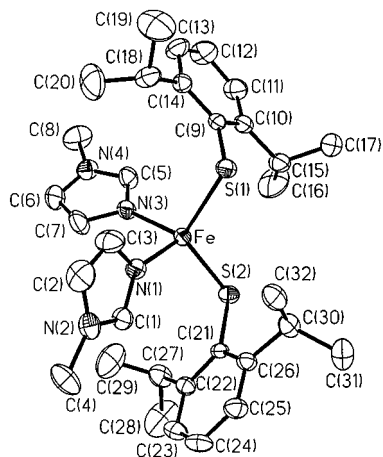


Figure 3. Structure and labeling of $\text{Fe}(\text{S}-2,6-i\text{-Pr}_2\text{C}_6\text{H}_3)_2(1\text{-MeIm})_2$, **1**. Thermal ellipsoids represent the 50% probability surfaces.

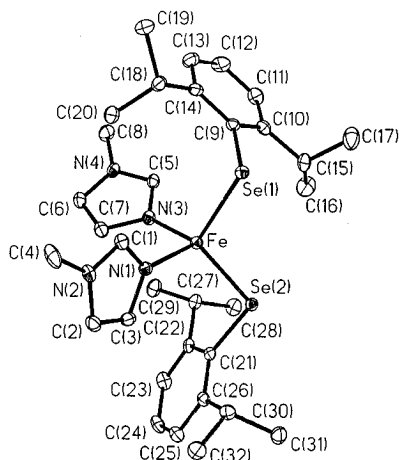


Figure 4. Structure and labeling of $\text{Fe}(\text{Se}-2,6-i\text{-Pr}_2\text{C}_6\text{H}_3)_2(1\text{-MeIm})_2$, **2**. Thermal ellipsoids represent the 33% probability surfaces.

and 2.4557(8) Å, and the Fe–N separations are 2.063(3) and 2.075(3) Å. The bond lengths and angles within the 1-MeIm ligands of **1** and **2** were compared with those for seven structures of 1-MeIm complexes of tetrahedral first-row transition metals (none of iron) from the Cambridge Structural Database.¹⁹ No significant differences between the parameters of the MeIm groups of **1** and **2** and the published structures were found.

One parameter that indicates the degree of distortion of a pseudotetrahedral complex is the dihedral angle between two planes each defined by the metal and two donor atoms. A regular tetrahedral coordination environment is characterized by having 90° dihedral angles. Using the two nitrogen atoms and the iron atom to define the first plane and the two chalcogen atoms and the iron atom to define the second plane, one calculates dihedral angles of 86.9° for **1** and 87.2° for **2**. The complex $\text{Fe}(\text{Se}-2,6-i\text{-Pr}_2\text{C}_6\text{H}_3)_2(\text{PMe}_2\text{Ph})_2$ with a dihedral angle of 81.4° is more distorted from a tetrahedral coordination geometry than are **1** and **2**. Similarly, one finds that the tetrachloroferrate(II) anion in $(\text{Me}_4\text{N})_2[\text{FeCl}_4]$ ²⁰ has one regular dihedral angle (90°) and two distorted dihedral angles of 69.4°. Distortions in this ion can be attributed to a compression due to the Jahn–Teller effect, whereas this need not be invoked for **1** and **2** because of the unsymmetrical coordination sphere.

A comparison of these structures with the other structurally characterized neutral four-coordinate thiolato transition metal

complexes is in order. The thiolato sulfur–metal–thiolato sulfur bond angles in $\text{Fe}(\text{S}-2,4,6-i\text{-Pr}_3\text{C}_6\text{H}_2)_2(\text{SC}(\text{NMe}_2)_2)_2$ (125.7(1)°),⁷ $\text{Fe}(\text{S}-2,4,6-\text{Me}_3\text{C}_6\text{H}_2)_2(\text{PMePh}_2)_2$ (133.6(1)°),⁸ $\text{Fe}(\text{S}-2,4-t\text{-Bu}_2\text{C}_6\text{H}_3)_2(\text{Ph}_2\text{PCH}_2\text{CH}_2\text{CH}_2\text{PPh}_2)$ (129.9(1)°),⁸ and $\text{Zn}(\text{SPh})_2(1\text{-MeIm})_2$ (128.47(4)°)²¹ and the Se–Fe–Se angles in $\text{Fe}(\text{Se}-2,6-i\text{-Pr}_2\text{C}_6\text{H}_3)_2(\text{PMe}_2\text{Ph})_2$ (130.3(1)°)⁹ and $\text{Fe}(\text{Se}-2,6-i\text{-Pr}_2\text{C}_6\text{H}_3)_2(\text{depe})$ (130.8(1)°)⁹ are much larger than those in both complexes **1** (116.5(1)°) and **2** (110.99(3)°). Wide S–M–S angles are also observed in $\text{Cd}(\text{S}-2,4,6-i\text{-Pr}_3\text{C}_6\text{H}_2)_2(1\text{-MeIm})_2$ (126.1(1)°)²² and $\text{Co}(\text{S}-2,4,6-i\text{-Pr}_3\text{C}_6\text{H}_2)_2(\text{py})_2$ (123.4(2)°).²³ The Br–Fe–Br angle is greater than the tetrahedral angle in the complex $\text{FeBr}_2(\text{PET}_3)_2$ (121.9°).⁴

Distortions from the tetrahedral geometry are generally attributed to steric effects. In the list above, there are examples of complexes with sterically demanding ligands which have regular structures and examples of distorted structures with ligands that have minimal steric demands. All of the structures with X–M–X (where X represents the anionic ligand) angles that approach the tetrahedral value also contain 1-MeIm coligands (in addition to **1** and **2**, there are $\text{Zn}(\text{S}-2,3,5,6-\text{Me}_4\text{C}_6\text{H}_2)_2(1\text{-MeIm})_2$ ²⁴ and $\text{Zn}(\text{S}-2,4,6-t\text{-Bu}_3\text{C}_6\text{H}_2)_2(1\text{-MeIm})_2$ ²⁵). But having 1-MeIm coligands does not guarantee a distortion-free structure as demonstrated by $\text{Zn}(\text{SPh})_2(1\text{-MeIm})_2$ ²¹ and $\text{Cd}(\text{S}-2,4,6-i\text{-Pr}_3\text{C}_6\text{H}_2)_2(1\text{-MeIm})_2$.²² From these data it appears that steric effects cannot account for the observed distortions. While crystal packing forces may account for these distortions, it is also possible that it is the electronic nature of the imidazole ligand which influences the geometry of these complexes.

Conclusion

Two neutral four-coordinate iron(II) 1-methylimidazole compounds with thiolate or selenolate donors have been prepared by metathesis of chloride ligands. Arenethiolate and -selenolate anions were generated by reduction of the corresponding diaryl disulfide or diselenide compounds. The 1-MeIm complexes reported here have distorted tetrahedral coordination geometry about iron. The E–Fe–E (E = chalcogen) angle is close to the 109.5° angle for tetrahedral coordination, while in the related phosphine complexes, this angle is greater (about 130°). This difference is attributed to the imidazole coligands or packing forces. The 1-MeIm complexes are air-sensitive and exhibit irreversible electrochemical behavior, which does not support an electron transport role for a biological analog. However, the rigid coordination geometry imposed by a metalloprotein could conceivably make the electrochemistry of an FeN_2S_2 site reversible.

Acknowledgment. We thank the Natural Sciences and Engineering Research Council of Canada for an operating grant to R.H.M. and the University of Toronto for a graduate scholarship to C.E.F. We also thank Mr. Nick Plavac of the NMR facility of this department for recording the ²H NMR spectra and Ontario Hydro for a gift of D₂O.

Supporting Information Available: Tables of crystallographic parameters, hydrogen atomic coordinates, thermal parameters, and bond distances and angles for **1** and **2** (11 pages). Ordering information is given on any current masthead page.

IC951222E

(19) Cambridge Structural Database, released April 1995. See: Allen, F. H.; Kennard, O.; Taylor, R. *Chem. Des. Autom. News* **1993**, 8, 31–37.

(20) Lauher, J. W.; Ibers, J. A. *Inorg. Chem.* **1975**, 14, 348–352.

(21) Wilker, J. J.; Lippard, S. J. *J. Am. Chem. Soc.* **1995**, 117, 8682–8683.

(22) Santos, R. A.; Gruff, E. S.; Koch, S. A.; Harbison, G. S. *J. Am. Chem. Soc.* **1990**, 112, 9257–9263.

(23) Corwin, D. T., Jr.; Gruff, E. S.; Koch, S. A. *J. Chem. Soc., Chem. Commun.* **1987**, 966–967.

(24) Corwin, D. T., Jr.; Koch, S. A. *Inorg. Chem.* **1988**, 27, 493–496.

(25) Bochmann, M.; Bwembya, G. C.; Grinter, R.; Powell, A. K.; Webb, K. J.; Hursthouse, M. B.; Malik, K. M. A.; Mazid, M. A. *Inorg. Chem.* **1994**, 33, 2290–2296.